*International Journal of Thermophysics, Vol. 18, No. 1, 1997*

# A Noncontact Method for Measuring Thermal Conductivity and Thermal Diffusivity of Anisotropic Materials

**M. Fujii,[1,2] S. C. Park,[1] T. Tomimura,[1] and X. Zhang[1]**

*Received March 21, 1996*

A noncontact method for measuring the thermal conductivity and thermal diffusivity of anisotropic materials is proposed. This method is based on the fact that the surface temperature variation with time depends on the thermal properties of the material when its surface is heated locally. The three-dimensional transient heat conduction equation in the material is solved numerically. The dimensionless average surface temperature variations are obtained along each principal axis; that is, the $x$ and $y$ axes. The relation between the dimensionless temperature and the Fourier number is expressed by a polynomial equation and used as a master plot, which is a basic relation to be compared with measured temperature variation. In the experiments, the material surface is heated with a laser beam and the surface temperature profiles are measured by an infrared thermometer. The measured temperature variations with time are compared with the master plots to yield the thermal conductivity $\lambda_x$ and thermal diffusivity $\alpha_x$ in the $x$ direction and the thermal conductivity ratio $E_{xy}(=\lambda_y/\lambda_x)$ simultaneously. To confirm the applicability and the accuracy of the present method, measurements were performed on multilayered kent-paper, vinyl chloride, and polyethylene resin film, whose thermal properties are known. From numerical simulations, it is found that the present method can measure the thermophysical properties $\lambda_x$, $\alpha_x$ and $E_{xy}$ within errors of $\pm 6$, $\pm 22$, and $\pm 5\%$, respectively, when the measuring errors of the peak heat flux, the heating radius, and the surface temperature rise are assumed to be within $\pm 2$, $\pm 3\%$, and $\pm 0.2$ K, respectively. This method could be applied to the measurement of thermophysical properties of biological materials.

**KEY WORDS:** anisotropic material; noncontact measurement method; thermal conductivity; thermal diffusivity.

[1] Institute of Advanced Material Study, Kyushu University, Kasuga, Fukuoka 816, Japan.
[2] To whom correspondence should be addressed.

## 1. INTRODUCTION

As anisotropic materials whose thermal conductivity and thermal diffusivity depend on directions, there are insulation materials, multilayered materials, biological materials, etc. In the fields of medical engineering and biotechnology, it is particularly important to perform an *in vivo* measurement of thermophysical properties of biological materials. It is very difficult to obtain accurate thermophysical properties by the conventional *invasive* method, because a living body reacts sensitively on such foreign substances as probes.

To overcome this problem, the authors have proposed a noncontact measurement method using a laser and an infrared thermometer, and established the simultaneous measuring technique of thermal conductivity and thermal diffusivity of isotropic materials and, further, examined errors in the measurements [1, 2]. The method is based on the fact that the surface temperature variation with time after step heating depends on the thermal properties of the material, therefore, by combining the laser heating with the surface temperature measurement by an infrared thermometer, a noncontact (i.e., *noninvasive*) measurement of thermophysical properties becomes possible.

In this paper, the method proposed for isotropic materials is extended to measure anisotropic materials by performing three-dimensional transient numerical simulation and by measuring the two-dimensional surface temperature distributions. The thermophysical properties of anisotropic materials such as multilayered kent-paper, vinyl chloride, and polyethylene resin film are measured. As for the kent-paper, the measured results are compared to those obtained by Takegoshi et al. [3] using the transient hot-wire method. Further, the validity of the present measurement method is confirmed, and the effects of the measurement errors of the peak heat flux, the heating radius, and the surface temperature rise on the accuracy of the thermophysical property evaluation are investigated quantitatively.

## 2. NUMERICAL ANALYSIS AND MEASURING PRINCIPLE

### 2.1. Physical Model and Basic Equations

In the present measurement method, the thermal conductivity and thermal diffusivity of a material are estimated simultaneously by fitting the measured surface temperature variation to that obtained numerically. In this section, a numerical analysis is described which clarifies the relation between the surface temperature variation and its thermophysical properties.

Figure 1 shows the physical model (two-layered model) and the coordinate system. Corresponding to the test material shown in Section 3, a black paint layer coated on its surface is considered. The rectangular prism ($2y_s$ long, $2x_s$ wide, and $z_s$ thick) of an anisotropic material is placed in still air of temperature $T_\infty$. The thermal conductivities and thermal diffusivities in the $x$, $y$, and $z$ directions are $\lambda_x$, $\lambda_y$, and $\lambda_z$ and $\alpha_x$, $\alpha_y$, and $\alpha_z$, respectively. The thin black paint layer of thickness $z_b$ has the thermal conductivity $\lambda_b$, the thermal diffusivity $\alpha_b$, and the emissivity $\varepsilon$. The black paint surface is locally heated with a laser beam. Taking account of the Gaussian distribution of the beam intensity, the heat flux distribution $q(r)$ is given as

$$q(r) = q_p \exp\{-2.3(r/r^*)^2\} \tag{1}$$

where $r^*$ is the heating radius, which is defined as the radius where the heat flux becomes 10% of the peak value at the beam center $q_p = q(0)$. Most part of the heat input is conducted through the paint layer and the material, and the rest is transferred back to the ambient by free convection ($q_c$) and radiation ($q_r$). The basic equations of three-dimensional transient

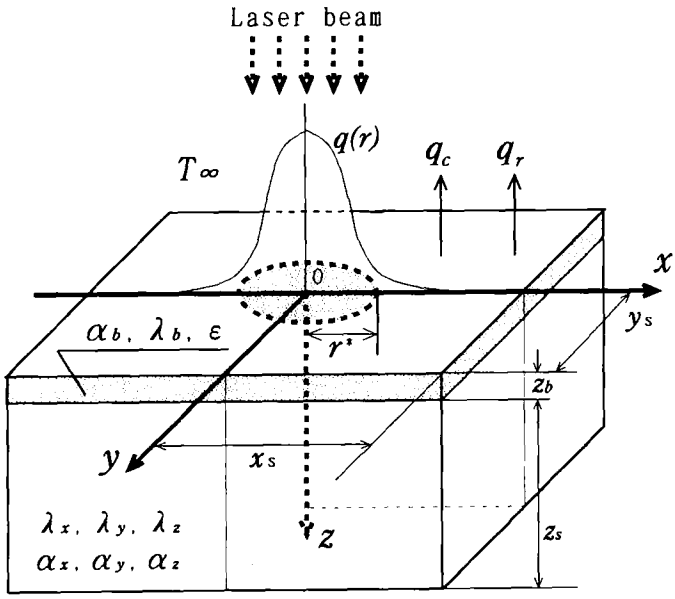


**Fig. 1.** Physical model and the coordinate system.

heat conduction for the black paint layer (subscript $b$) and the anisotropic material (subscript $s$) are written in dimensionless form as

$$\frac{\partial \Theta_b}{\partial \mathrm{Fo}} = P_{xx}\left(\frac{\partial^2 \Theta_b}{\partial X^2} + \frac{\partial^2 \Theta_b}{\partial Y^2} + \frac{\partial^2 \Theta_b}{\partial Z^2}\right) \tag{2}$$

$$\frac{\partial \Theta_s}{\partial \mathrm{Fo}} = \frac{\partial^2 \Theta_s}{\partial X^2} + E_{xy}\frac{\partial^2 \Theta_s}{\partial Y^2} + E_{xz}\frac{\partial^2 \Theta_s}{\partial Z^2} \tag{3}$$

The initial conditions are given by

$\mathrm{Fo} = 0$:

$$0 \leqslant X \leqslant X_s, \quad 0 \leqslant Y \leqslant Y_s, \quad 0 \leqslant Z \leqslant Z_b; \quad \Theta_b = 0$$

$$0 \leqslant X \leqslant X_s, \quad 0 \leqslant Y \leqslant Y_s, \quad Z_b \leqslant Z \leqslant Z_b + Z_s; \quad \Theta_s = 0 \tag{4}$$

and the boundary conditions are given by

$\mathrm{Fo} > 0$:

$$0 < X < X_s, \quad 0 \leqslant Y \leqslant Y_s, \quad Z = 0;$$

$$-P_{zx}\frac{\partial \Theta_b}{\partial Z} = \exp(-2.3R^2) - \mathrm{Bi}\,\Theta_w - Rc\Theta_w$$

$$0 < X \leqslant X_s, \quad 0 < Y \leqslant Y_s, \quad Z = Z_b + Z_s; \quad \frac{\partial \Theta_s}{\partial Z} = 0$$

$$0 < X \leqslant X_s, \quad Y = 0, Y_s, \quad 0 < Z \leqslant Z_b; \quad \frac{\partial \Theta_b}{\Theta Y} = 0$$

$$0 < X \leqslant X_s, \quad Y = 0, Y_s, \quad Z_b < Z \leqslant Z_b + Z_s; \quad \frac{\partial \Theta_s}{\partial Y} = 0$$

$$X = 0, X_s, \quad 0 < Y \leqslant Y_s, \quad 0 < Z \leqslant Z_b; \quad \frac{\partial \Theta_b}{\partial X} = 0$$

$$X = 0, X_s, \quad 0 < Y \leqslant Y_s, \quad Z_b < Z \leqslant Z_b + Z_s; \quad \frac{\partial \Theta_s}{\partial X} = 0$$

$$0 < X \leqslant X_s, \quad 0 < Y \leqslant Y_s, \quad Z = Z_b;$$

$$P_{zz}\frac{\partial \Theta_b}{\partial Z} = \frac{\partial \Theta_s}{\partial Z}, \quad \Theta_b = \Theta_s \tag{5}$$

The dimensionless variables are defined by

$$\Theta = \frac{T - T_\infty}{q_p r^* / \lambda_x}, \qquad \mathrm{Fo} = \frac{\alpha_x t}{r^{*2}}, \qquad X = \frac{x}{r^*}, \qquad Y = \frac{y}{r^*}, \qquad Z = \frac{z}{r^*}, \qquad R = \frac{r}{r^*}$$

$$P_{\lambda x} = \frac{\lambda_h}{\lambda_x}, \qquad P_{\alpha x} = \frac{\alpha_h}{\alpha_x}, \qquad P_{\lambda z} = \frac{\lambda_h}{\lambda_z}, \qquad E_{xy} = \frac{\lambda_y}{\lambda_x}, \qquad E_{xz} = \frac{\lambda_z}{\lambda_x}$$

$$\mathrm{Bi} = \frac{hr^*}{\lambda_x}, \qquad Rc = \frac{4T_\infty^3 \varepsilon \sigma r^*}{\lambda_x} \tag{6}$$

In the above equations, $\Theta$ is the dimensionless temperature, $\Theta_w$ $[= \Theta_h(\mathrm{Fo}, R, 0)]$ the dimensionless surface temperature, $T$ the absolute temperature, $t$ the time after step heating, and Fo the corresponding Fourier number, $X$, $Y$, $Z$, and $R$ are the dimensionless coordinates, $P_{\lambda x}$ and $R_{\lambda z}$ are the ratios of thermal conductivity of the black paint to those of the material in the $x$ and $z$ directions, respectively, $P_{\alpha x}$ is the similar ratio of thermal diffusivities, $E_{xy}$, and $E_{xz}$ are the ratios of thermal conductivities in the respective directions, and Bi is the Biot number, $h$ the heat transfer coefficient, $Rc$ the conduction-radiation parameter, and $\sigma$ the Stefan–Boltzmann constant.

## 2.2. Parameters

The basic equations are solved numerically by the finite difference method under the previous initial and boundary conditions. In the present calculations, the ranges of the dimensionless parameters $P_{\alpha x}$, $E_{xy}$, and $E_{xz}$ in Eqs. (2) and (3), and $P_{\lambda x}$, $P_{\lambda z}$, $Z_h$, Bi, and $Rc$ in the initial and boundary conditions Eqs. (4) and (5), are chosen as

$$P_{\lambda x} = 1, 6, 15, \qquad P_{\alpha x} = 1, 5, 10, 15, \qquad P_{\lambda z} = P_{\lambda x}$$

$$E_{xy} = 0.1, 0.2, 0.5, 1, 2, 4, 6, \qquad E_{xz} = 1$$

$$\mathrm{Bi} = 0.02 \sim 0.11, \qquad Rc = (0.66 \sim 4.0) \times 10^{-2}, \qquad Z_h = 3.5 \times 10^{-2}$$

where the ranges of $P_{\alpha x}$ and $P_{\lambda x}$ are determined by considering the values of $\lambda_h = 1.89\ \mathrm{W \cdot m^{-1} \cdot K^{-1}}$ and $\alpha_h = 1.09 \times 10^{-6}\ \mathrm{m^2 \cdot s^{-1}}$ obtained from the previous measurements [4], and also those of the present test materials and the living tissues [5], as

$$\lambda_x = 0.1 \sim 0.6\ \mathrm{W \cdot m^{-1} \cdot K^{-1}}, \qquad \alpha_x = (0.1 \sim 0.5) \times 10^{-6}\ \mathrm{m^2 \cdot s^{-1}}$$

The values of Bi, $Rc$, and $Z_h$ are determined from the relevant values of $h = 15\ \mathrm{W \cdot m^{-2} \cdot K^{-1}}$, $r^* = 0.71 \times 10^{-3}\ \mathrm{m}$, $T_\infty = 293\ \mathrm{K}$, $\varepsilon = 0.98$, and

$z_b = 25 \times 10^{-6}$ m. It should be noted that only the case of $E_{xz} = 1$ is treated in the present paper.

### 2.3. Measuring Principle

To establish a simple procedure for evaluating the thermal conductivity and thermal diffusivity from the numerical results, a unique relation between $\Theta_w$ and Fo as a master plot which is independent of the parameters Bi and $Rc$ should be obtained. For this purpose, similar to the previous study [1, 2], the following dimensionless surface temperature,

$$\Theta_{wn} = \frac{T_w - T_\infty}{q_n r^*/\lambda_x} = \frac{\Delta T_w}{q_n r^*/\lambda_x} = \Theta_w \frac{q_p}{q_n} \tag{7}$$

is introduced by replacing the peak heat flux $q_p$ included in $\Theta_w$ with an average net heat flux defined by

$$q_n = \frac{1}{\pi r^{*2}} \int_0^{r^*} [q_p \exp\{-2.3(r/r^*)^2\} - h(T_w - T_\infty) - \varepsilon\sigma(T_w^4 - T_\infty^4)] \, 2\pi r \, dr \tag{8}$$

where $T_w$ is the surface temperature of black paint. The redefined dimensionless surface temperature $\Theta_{wn}$ is confirmed to be almost independent of Bi and $Rc$ for the ranges shown in the previous section.

When a material is anisotropic, the isotherms on the surface show not concentric circle but ellipsoid. In this case, the $X$ and $Y$ axes are chosen to coincide with the long and short axes of the ellipsoid, respectively. Then the following dimensionless parameters are introduced.

$$I_{th-X} = \frac{1}{\pi R^{*2}} \int_0^{R^*} \Theta_{wn-X} 2\pi R \, dR \tag{9}$$

$$I_{th-Y} = \frac{1}{\pi R^{*2}} \int_0^{R^*} \Theta_{wn-Y} 2\pi R \, dR \tag{10}$$

Equations (9) and (10) are the superficial average temperatures which would be defined under the assumption that the respective temperature distribution in the $X$ or $Y$ direction is the same as that for an isotropic material.

Figure 2 shows an example of time variation of $I_{th-X}$ and $I_{th-Y}$. The relations also are found to be independent of Bi and $Rc$ in the rages of the present calculations. The relations, therefore, can be used as the master plots for the present measurement method. Since the larger fraction of heat

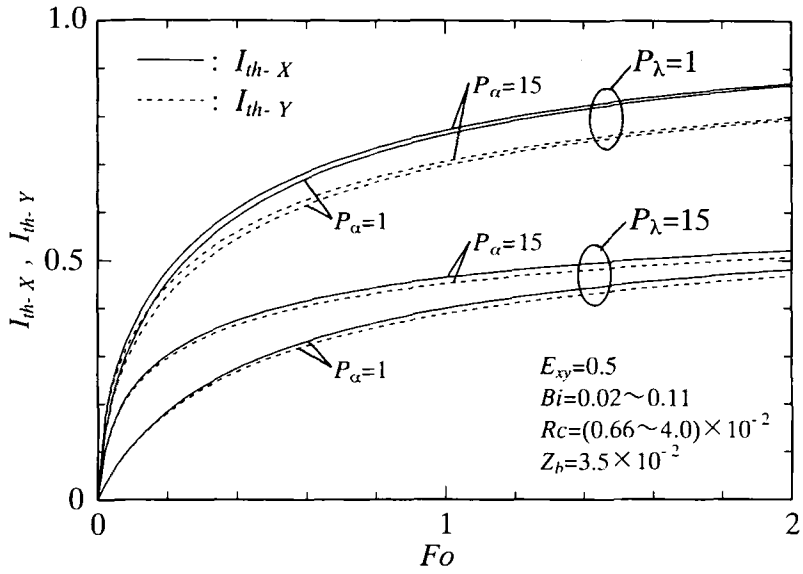


**Fig. 2.** Dimensionless mean surface temperature variations.

flows in the $X$ direction for the case of $E_{xy}=0.5(\lambda_y=0.5\lambda_x)$ shown in Fig. 2, the average surface temperature $I_{th-X}$ becomes high compared with $I_{th-Y}$. With increasing $P_\lambda$, however, the lateral heat flows through the black paint layer increases, and therefore, the difference between $I_{th-X}$ and $I_{th-Y}$ is reduced for $P_\lambda=15$.

The change of $I_{th-Y}$ with time is approximated with the polynomial expression $I_{th-Y}=G(\mathrm{Fo})$. Here, the integration of the function $G(\mathrm{Fo})$ for $\mathrm{Fo}=0\sim\mathrm{Fo}$ is defined as

$$A_{th-Y}=\int_0^{\mathrm{Fo}} I_{th-Y}\,d\mathrm{Fo}=\int_0^{\mathrm{Fo}} G(\mathrm{Fo})\,d\mathrm{Fo} \tag{11}$$

From the measurements, on the other hand, corresponding to Eqs. (9), (10), and (11), the following quantities are introduced from the measured surface temperature distributions along the $x$ and $y$ axes $\Delta T_{w-x}$ and $\Delta T_{w-y}$, at time $t$.

$$i_{ex-x}=\frac{1}{\pi r^{*2}}\int_0^{r^*}\frac{\Delta T_{w-x}}{q_n}2\pi r\,dr \tag{12}$$

$$i_{ex-y}=\frac{1}{\pi r^{*2}}\int_0^{r^*}\frac{\Delta T_{w-y}}{q_n}2\pi r\,dr \tag{13}$$

Also, by integrating the polynomial approximation expression $t_{ex-y} = g(t)$ for $t = 0 \sim t$, the quantity

$$a_{ex-y} = \int_0^t i_{ex-y}\, dt \doteqdot \int_0^t g(t)\, dt \tag{14}$$

is defined.

The estimation method of the thermal conductivity and thermal diffusivity of anisotropic materials using Eqs. (9)–(14) is shown in Fig. 3. The process is as follows:

(1) By selecting a proper time after step heating $t_0$, the values of $i_{ex-x}$ and $i_{ex-y}$ and its integration value $a_{ex-y}$ at $t = t_0$ are calculated. The

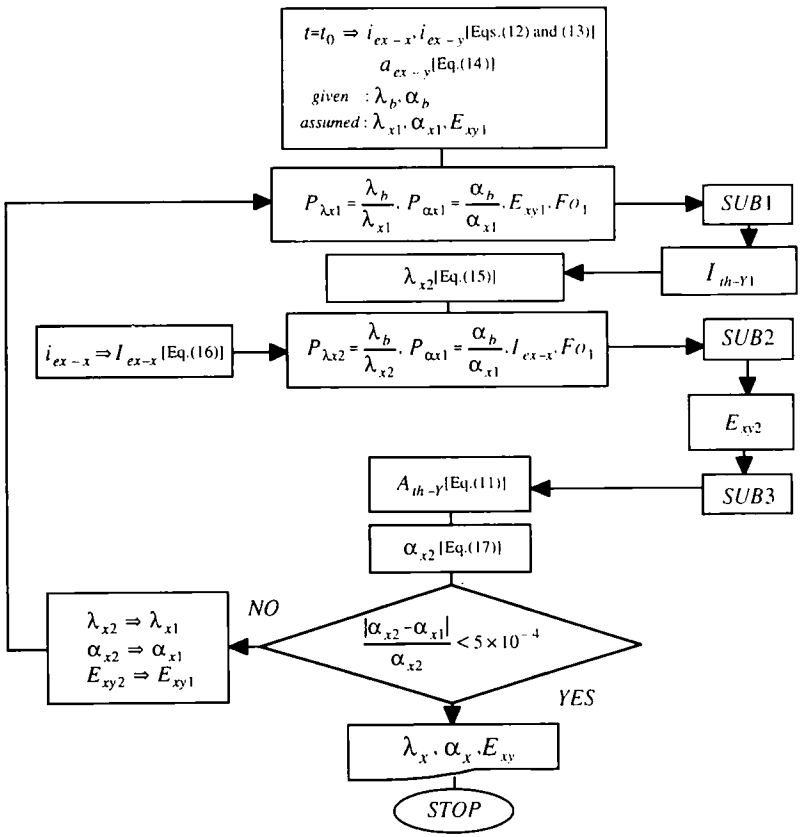


**Fig. 3.** Flowchart for evaluating thermal conductivity and thermal diffusivity of anisotropic materials.

thermal conductivity and thermal diffusivity in the $x$ direction $\lambda_{x1}$, and $\alpha_{x1}$ and the ratio of thermal conductivities in the $x$ and $y$ direction $E_{xy1}$ of the material are assumed.

(2) The thermal conductivity and thermal diffusivity ratios of the black paint to the material $P_{\lambda x1}$ and $P_{\alpha x1}$ are determined from the assumed values $\lambda_{x1}$ and $\alpha_{x1}$ and the given thermophysical properties of the black paint layer $\lambda_b$ and $\alpha_b$. The Fourier number $\mathrm{Fo}_1$ corresponding to $\alpha_{x1}$ and the time $t_0$ is also determined.

(3) Using the program SUB1 where the relations between $I_{th-y}$ and Fo are given for each combination of the parameters $P_\lambda$, $P_\alpha$, and $E_{xy}$, the dimensionless average surface temperature $I_{th-y1}$ at $P_{\lambda x1}$, $P_{\alpha x1}$, $E_{xy1}$, and $\mathrm{Fo}_1$ is obtained by interpolation.

(4) Thus the obtained $I_{th-y1}$ and the measured value $i_{ex-y}$ are substituted into the relation,

$$\lambda_{x2}=\frac{I_{th-y1}r^*}{i_{ex-y}} \tag{15}$$

to obtain the first approximate value of thermal conductivity $\lambda_{x2}$.

(5) Using $\lambda_{x2}$ the measured value of $i_{ex-x}$ is transformed into dimensionless form as

$$I_{ex-x}=\frac{i_{ex-x}\lambda_{x2}}{r^*} \tag{16}$$

(6) Similar to the third step, using the program SUB2 in which the relations between $I_{th-x}$ and $E_{xy}$ are given at the fixed values of $P_{\lambda x}$, $P_{\alpha x}$, and Fo, the first approximate value of the thermal conductivity ratio $E_{xy2}$ is determined so that $I_{th-x}$ coincides with $I_{ex-x}$.

(7) Through the program SUB3, the polynomial expression $I_{th-y}=G(\mathrm{Fo})$ for $P_{\lambda x2}$, $P_{\alpha x1}$, and $E_{xy2}$ is obtained by interpolation. Then the integral $A_{th-y}$ is calculated from Eq. (11) for $\mathrm{Fo}=0\sim\mathrm{Fo}$.

(8) The measured value $a_{ex-y}$ and thus the obtained $A_{th-y}$ are substituted into the relation,

$$\alpha_{x2}=\frac{r^{*3}}{a_{ex-y}\lambda_{x2}}A_{th-y} \tag{17}$$

to obtain the first approximate value of thermal diffusivity $\alpha_{x2}$.

(9) Until the relative error in thermal diffusivity satisfies a given convergent criterion, the steps from 2 to 8 are repeated by replacing $\lambda_{x1}$,

$\alpha_{x1}$, and $E_{xy1}$ with $\lambda_{x2}$, $\alpha_{x2}$, and $E_{xy2}$. Finally, the thermal conductivity and thermal diffusivity in the $y$ direction $\lambda_y (=E_{xy}\lambda_x)$, and $\alpha_y (=E_{xy}\alpha_x)$ are estimated from the converged values of $\lambda_x$, $\alpha_x$, and $E_{xy}$.

## 3. MEASUREMENTS

A schematic diagram of the measuring system is shown in Fig. 4. The system consists of an argon laser (wavelength, 514.5 nm) (4) with a shutter (3), an infrared thermometer system (6–9), and a test material (1). The material surface is heated directly by the argon laser. The intensity distribution of the laser beam is confirmed to be Gaussian, and at the same time, the heating radius $r^*$ is determined to be 0.71 mm by measuring the relative intensity through a 10-$\mu$m-diameter pin hole with a photodiode [3]. The laser output is adjusted by a power controller (5), and its values before and after a measurement are checked using a power meter (2) and a digital

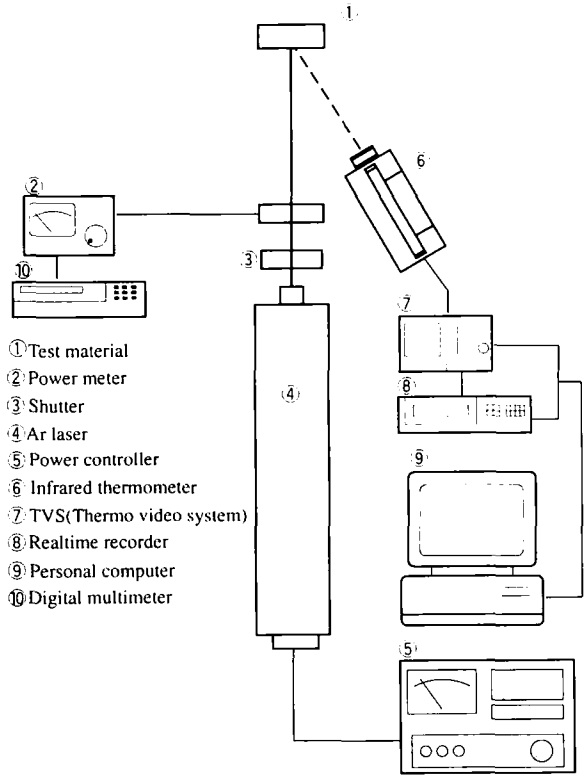


Fig. 4. Schematic diagram of the measuring system.

multimeter (10). The power meter has about 0.1-mW resolution. In the present measurement, the laser output is adjusted to about 20 mW, and under this condition, the surface central temperature rise at 3 s after step heating becomes 13–15 K. The variation of laser power before and after a measurement is within $\pm 1\%$.

The infrared thermometer system can measure the two-dimensional surface temperature distributions and, also, record the data every 1/30 s. The temperature range of 20–40°C is selected in the measurement. In this case, resolution of the temperature measurements is estimated to be about 0.1 K, however, some fluctuations of about 0.2 K are observed. The space resolution is estimated to be 0.1 mm, when the focal length of the thermometer is set to be 0.1 m as in the present case.

Figure 5 shows a schematic diagram of the sample as an anisotropic material. The samples used in the present study are multilayered sheets of kent-paper, vinyl chloride, and polyethylene resin film. The materials are 30 mm long, 20 mm high, and 13–16 mm thick. To minimize the effect of the laser beam reflection, a thin black paint layer is coated on the central part ($10 \times 10$ mm$^2$) of the material surface. The layer is rubbed with a glass rod to have a $24 \pm 2$-$\mu$m thickness. Such a degree of nonuniformity in thickness is confirmed to have no effect on the accuracy of the measurement. The absorptivity of the paint layer for argon laser beam is estimated to be 0.73 under such surface conditions [4]. The detail of the test materials is listed in Table I. The materials, Kent-a, -b, and -c, are composed of 60 sheets of kent-paper. As for Kent-d, each sheet is pasted together with a 50-$\mu$m-thick acrylic double-faced adhesive tape having the thermal conductivity $\lambda = 0.21$ W $\cdot$ m$^{-1}$ $\cdot$ K$^{-1}$ [6]. The materials, V.C. and P.E., are composed of 115 sheets of vinyl chloride resin film ($\lambda = 0.15$–$0.21$ W $\cdot$ m$^{-1}$ $\cdot$ K$^{-1}$ [6]) and 150 sheets of polyethylene resin film ($\lambda = 0.34$–$0.53$ W $\cdot$ m$^{-1}$ $\cdot$ K$^{-1}$ [6]), respectively.

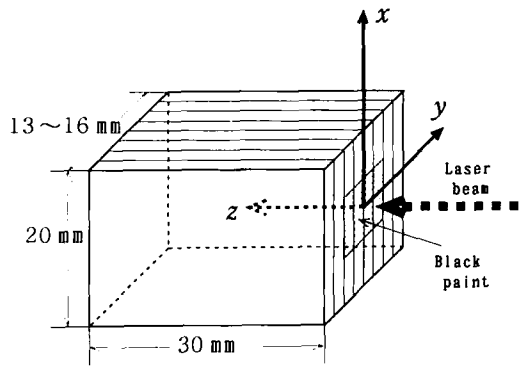


Fig. 5. Schematic diagram of the multilayered test material.

**Table I.** Parameters of the Multilayered Test Material

| Test material | Thickness of paper or film (mm) | Number of sheets of paper or film | Bulk density ($kg \cdot m^{-3}$) |
|---|---|---|---|
| Kent-a | $0.227 \pm 0.003$ | 60 | 911 |
| Kent-b | $0.224 \pm 0.003$ | 60 | 916 |
| Kent-c | $0.228 \pm 0.003$ | 60 | 915 |
| Kent-d | $0.226 \pm 0.003$ | 60 | 950 |
| V.C. | $0.115 \pm 0.006$ | 115 | 1300 |
| P.E. | $0.095 \pm 0.002$ | 150 | 970 |

The measurements were performed six times for each material at an ambient temperature of 22–23°C and a relative humidity of 70–80%. In the data processing, the coordinate system is taken as that shown in Fig. 5, that is, the $x$ axis to be parallel to the paper or film edge direction.

## 4. RESULTS AND DISCUSSION

Figure 6 shows an example of the measured variations of $i_{ex\cdot x}$ and $i_{ex\cdot y}$ which are defined by Eqs. (12) and (13) as the variables corresponding to the average surface temperatures. As the larger fraction of heat flows along the paper or film edge direction, that is, in the $x$ direction, $i_{ex\cdot x}$ is always higher than $i_{ex\cdot y}$. The fluctuations observed in the figure

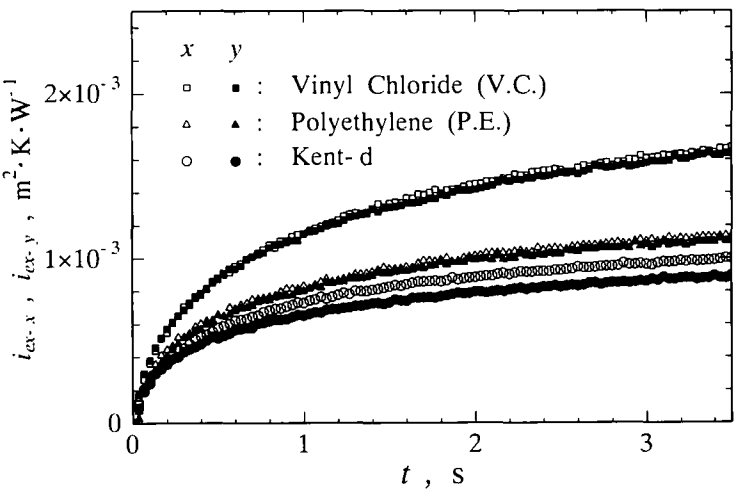


**Fig. 6.** Measured mean surface temperature variations.

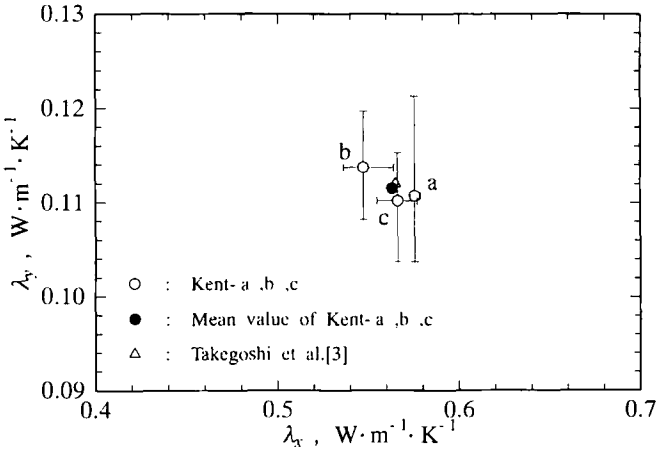


Fig. 7. Comparison of measured thermal conductivities with literature values. ( ) Kent-b, -b, and -c; (●) mean value of Kent-a, -b, and -c; (△) value measured by Takegoshi et al. [3] with the transient hot-wire method.

are eliminated by approximating $i_{ex}$ and $i_{ex}$ with polynomial expressions of time $t$, and the expressions are used for evaluation process described previously.

In Fig. 7, the measured thermal conductivities $\lambda_x$ and $\lambda_y$ for Kent-a, -b, and -c are compared to those measured by Takegoshi et al. [3] with the transient hot-wire method. They used a sample composed of 60 sheets of kent-paper 200 mm long, 200 mm wide, and about 0.2 mm thick. The lines attached to each symbol show the range of scatter in each six measurements. As shown in Fig. 7, the mean value of Kent-a, -b and -c agrees well with those obtained by Takegoshi et al.

The measured results of $\lambda_x$, $\lambda_y$, $\alpha_x$, $\alpha_y$, and $E_{xy}$ of the present multilayered test materials are listed in Table II. Compared with Kent-a, -b, and -c, the thermal conductivity of Kent-d is lower in the $x$ direction, and higher in the $y$-direction. The reason may be attributed to the effect of adhesive tape between the sheets of paper, and explained by considering the following equivalent thermal conductivities

$$\lambda_{x\ eq} = \frac{\lambda_x \delta_s + \lambda_t \delta_t}{\delta_s + \delta_t} \tag{18}$$

$$\lambda_{y\ eq} = \frac{\delta_s + \delta_t}{(\delta_s/\lambda_y) + (\delta_t/\lambda_t)} \tag{19}$$

**Table II.** Measured Thermophysical Properties[a]

| | $\lambda_x$ | $\lambda_y$ | $\alpha_x$ | $\alpha_y$ | $E_{xy}$ |
|---|---|---|---|---|---|
| Kent-a | 0.576 | 0.111 | 0.415 | 0.080 | 0.192 |
| Kent-b | 0.547 | 0.114 | 0.332 | 0.069 | 0.208 |
| Kent-c | 0.566 | 0.110 | 0.392 | 0.076 | 0.195 |
| Mean value of Kent-a, -b, -c | 0.563 | 0.111 | 0.380 | 0.075 | 0.198 |
| Kent-d | 0.497 | 0.155 | 0.222 | 0.069 | 0.311 |
| V.C. | 0.200 | 0.122 | 0.120 | 0.073 | 0.608 |
| P.E. | 0.342 | 0.275 | 0.141 | 0.113 | 0.803 |

[a] Thermal conductivity, $\lambda$, in $W \cdot m^{-1} \cdot K^{-1}$ and thermal diffusivity, $\alpha$, in $10^{-6} m \cdot s^{-1}$.

These relations are derived from one-dimensional heat conduction model in each direction for the multilayered material where the kent-paper and the adhesive tape are piled up alternately. By using the values $\delta_t = 0.05 \times 10^{-3}$ m and $\lambda_t = 0.2\ W \cdot m^{-1} \cdot K^{-1}$ for the adhesive tape, and the mean values $\delta_s = 0.226 \times 10^{-3}$ m, $\lambda_x = 0.563\ W \cdot m^{-1} K^{-1}$, and $\lambda_y = 0.111\ W \cdot m^{-1} \cdot K^{-1}$ for kent-paper, the equivalent values of $\lambda_{x\ eq} = 0.499\ W \cdot m^{-1} \cdot K^{-1}$ and $\lambda_{y-eq} = 0.121\ W \cdot m^{-1} \cdot K^{-1}$ are obtained from Eqs. (18) and (19), respectively. Although thus estimated values do not coincide perfectly with the measured values of Kent-d, the effect of the adhesive tape may be estimated well with these equations.

In order to examine the validity of the present method, the numerical simulations are performed again by using the measured thermophysical properties. The recalculated results are compared with the measured surface temperatures in dimensionless forms. Figure 8 shows the surface temperature profiles along the $x$ and $y$ axes of the kent-paper at 3 s after step heating. The variables $I_{th}$ and $I_{ex}$ are plotted against Fo in Fig. 9. In these figures, the lines and the symbols represent the recalculated and the measured results, respectively. It is seen that these recalculated and measured agree very well. The fact confirms that the present curve-fitting method is performed satisfactorily.

Assuming that the thermal conductivity $\lambda_b$, the thermal diffusivity $\alpha_b$, and the thickness $z_b$ of the black paint layer are exactly known, the accuracy of the present method is estimated and the errors are listed in Table III. These are obtained from numerical simulations for the effects of the measurement errors of the peak heat flux $q_p$, the heating radius $r^*$, and the surface temperature rise $\Delta T_w$. The errors of $q_p$, $r^*$, and $\Delta T_w$ are

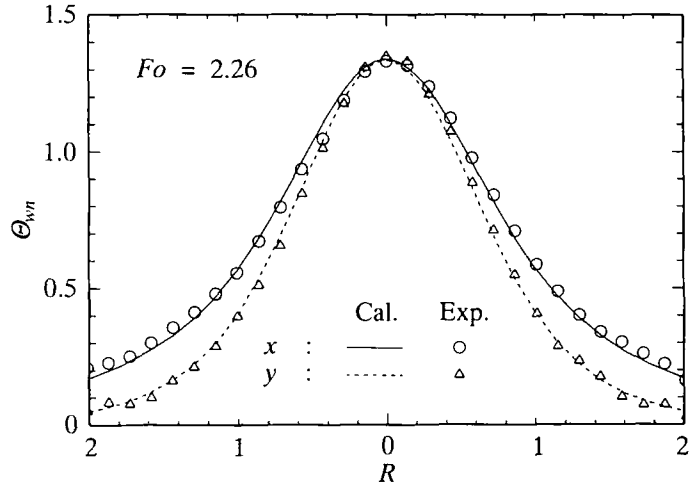


Fig. 8. Surface temperature profiles at 3 s after step heating.

estimated from the variations of the laser output before and after a measurements ($\pm 1\%$), the space resolution of the pin hole (20 $\mu$m) and the temperature fluctuations of the infrared thermometer every 1/30-s measurement ($\pm 0.2$ K), respectively. Therefore, the errors in $r^*$ and $\Delta T_w$ are overestimated, especially for the latter, because the maximum fluctuation 0.2 K is uniformly added to or subtracted from the surface temperature at

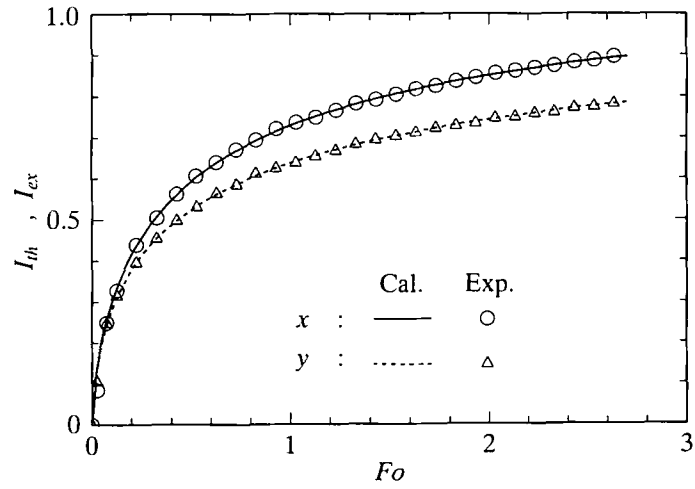


Fig. 9. Dimensionless mean surface temperature variations.

Table III. Estimates of Errors

| Measured quantity | Measuring error | Error (%) | | |
|---|---|---|---|---|
| | | $\lambda_x$ | $\alpha_x$ | $E_{xy}$ |
| $q_p$ (W·m$^{-2}$) | 2% | 2.4 (2.4) | 0.23 (0.28) | 1.0 (1.0) |
| $r^*$ (m) | 3% | 3.18 (3.14) | 8.7 (8.7) | 1.2 (1.2) |
| $\Delta T_w$ (K) | 0.2 K | 0 (0.1) | 12.9 (45) | 2.3 (5.0) |
| Total error (%) | | 6 (6) | 22 (54) | 5 (7) |

every measurements. In each column of $\lambda_x$, $\alpha_x$, and $E_{xy}$, the errors are indicated for two cases, that is, one for maximum temperature rise at 3 s after heating at $\Delta T_c \fallingdotseq 13$ K and the other for $\Delta T_c \fallingdotseq 5$ K (in parentheses). The latter is estimated for the purpose of the application of this method to the thermophysical property measurement of biological materials. The accuracy of $\lambda_x$ depends largely on the accuracy of the measurement of $q_p$ and $r^*$. As for $\alpha_x$, the errors of $r^*$ and $\Delta T_w$ are much more significant. In the case of $\Delta T_c \fallingdotseq 5$ K, the accuracy of $\lambda_x$ is the same for $\Delta T_c \fallingdotseq 13$ K. The accuracy of $\alpha_x$, however, remarkably reduces, since the relative error of $\Delta T_w$ to $\Delta T_c$ becomes large.

## 5. CONCLUSIONS

The noncontact method for measuring the thermal conductivity and thermal diffusivity proposed for isotropic materials is extended to anisopropic materials. The major conclusions are as follows:

(1) From the numerical simulations using the estimated thermophysical properties and comparisons with the measured surface temperatures, the validity of the present measurement method is confirmed. As for the kent-paper, the measured results agree well with those obtained by Takegoshi et al. [3] using the transient hot-wire method.

(2) It is clarified that the present method can measure the thermal conductivity $\lambda_x$, the thermal diffusivity $\alpha_x$, and the anisotropic ratio $E_{xy}$ within errors of $\pm 6$, $\pm 22$, and $\pm 5$% respectively, for the surface central temperature rise at 3 s after step heating at $\Delta T_c \fallingdotseq 13$ K.

(3) From the error estimation for the case of $\Delta T_c \fallingdotseq 5$ K, the method is found to be applicable at least for thermal conductivity measurements of biological materials.

## ACKNOWLEDGMENTS

The authors wish to acknowledge the valuable suggestions and discussion offered by Professor T. Fujii of Toa University. Mr. K. Hamano gratefully assisted in the fabrication of the apparatus and took part in performing the experiments.

## REFERENCES

1. M. Fujii, T. Tomimura, X. Zhang, and S. Park, *Thermophysical Properties* (International Academic, Beijing, 1992), pp. 120–125.
2. M. Fujii, S. Park, T. Tomimura, and X. Zhang, *Netsu Bussei* (*Jpn. J. Thermophys. Prop.*) **9** (4):231 (1995).
3. E. Takegoshi, S. Imura, T. Takenaka, and Y. Hirasawa, *Trans. Jpn. Soc. Mech. Eng.* (*B*) **48** (433):1743 (1982).
4. M. Fujii, S. Park, T. Tomimura, and X. Zhang, *Eng. Sci. Rep. Kyushu Univ.* (*Kyushu Daigaku Sogorikogaku Kenkyuka Hokoku*) **17** (1):23 (1995).
5. H. F. Bowman, E. G. Cravalho, and M. Woods, *Annu. Rev. Biophys. Bioeng.* **4**:43 (1975).
6. *JSTP Thermophysical Properties Hand Book* (Yokendo, Tokyo, 1990), pp. 272–273.